



# The deeply embedded starburst in SBS 0335-052

L. K. Hunt<sup>1</sup>, L. Vanzì<sup>2</sup>, T. X. Thuan<sup>3</sup>

<sup>1</sup> CAISMI-CNR, Largo E. Fermi 5, 50125 Firenze - ITALY email: hunt@arcetri.astro.it

<sup>2</sup> European Southern Observatory (ESO), Alonso de Cordova 3107, Santiago - CHILE  
email: lvanzi@eso.org

<sup>3</sup> Astronomy Department, University of Virginia, Charlottesville, VA 22903 - U.S.A. email: txt@virginia.edu

Received ; accepted

**Abstract.** We present  $4\mu\text{m}$  ISAAC imaging and spectroscopy of the extremely metal-poor dwarf galaxy SBS 0335-052, aimed at a better understanding of the dust in this low-metallicity galaxy. The  $4\mu\text{m}$  emission turns out to be very compact, confined to the brightest pair of Super Star Clusters (SSCs). The  $Ks-L'$  color is extremely red, and the  $L'$  emission is consistent with the extrapolation of the ISO mid-infrared spectral energy distribution (SED). From hydrogen recombination lines and a fit to the near-/mid-infrared SED, we confirm a visual extinction of  $\gtrsim 15$  mag. Our data suggest that the sites of the optical and infrared emission are distinct: the optical spectral lines come from an almost dustless region with a high star formation rate and a few thousand OB stars. This region lies along the line-of-sight to a very dusty central star cluster in which there are more than three times as many massive stars, completely hidden in the optical. From the extinction, we derive an upper limit for the dust mass of  $10^5 M_{\odot}$  which could be produced by recent supernovae.

**Key words.** Galaxies: dwarf; Galaxies: ISM; Galaxies: starburst; Galaxies: star clusters; Galaxies: individual: SBS0335-052

## 1. Introduction

With an abundance of  $Z_{\odot}/41$ , SBS 0335-052 is the lowest-metallicity galaxy in the Second Byurakan Survey (Markarian et al. 1983), and the second lowest known after I Zw 18. Because of its low optical luminosity ( $M_B = -16.7$ ), its small size (3-4 kpc diameter), and its strong narrow HII-region-like emission lines, it is classified as a Blue Compact Dwarf (BCD) galaxy (Thuan et al. 1997). SBS 0335-052 hosts an exceptionally powerful episode of star formation that, according to Thuan et al. (1997), occurs mainly in six Super-Star Clusters (SSCs) not older than 25 Myr. ISO observations of SBS 0335-052 (Thuan et al., 1999 - hereafter TSM) have revealed copious mid-infrared emission (the spectrum peaks at  $14\mu\text{m}$ ) and a spectral energy distribution (SED) that is well fit from 7 to  $17\mu\text{m}$  by a heavily absorbed modified blackbody. From their fit TSM deduce an optical extinction in the range 19-21 mag and speculate that most of the star formation in SBS 0335-052 may be optically obscured.

To better probe the extinction in SBS 0335-052, Vanzì et al. (2000 - hereafter VHTI) obtained a high spatial resolution image in the  $Ks$  band and a near-infrared (NIR)

spectrum. Comparing these observations with HST images and optical ground-based spectroscopy, they found no clear evidence for high extinction in SBS 0335-052. However, NIR colors suggest that a fraction of the  $K$ -band flux is produced by dust. Indeed that fraction is consistent with the mid-infrared SED, and a fit of the combined from 2 to  $15\mu\text{m}$  spectrum gave a visual extinction  $A_V \sim 12$  magnitudes (VHTI).

To determine the nature of the dust, unexpected in such a low-metallicity object, we have targeted SBS 0335-052 at  $4\mu\text{m}$  to obtain, for the first time, spatially resolved imaging at a thermal wavelength. At the same time, the low extinction at  $4\mu\text{m}$  enables us to probe the ionized gas via the  $\text{Br}\alpha$  recombination line.

## 2. Observations

We obtained a long-wavelength ( $2.7 - 4.2\mu\text{m}$ ) low-resolution ( $R=360$ ) spectrum of SBS 0335-052 with ISAAC at the ESO-ANTU (UT1). The observations were acquired in three different occasions on October 9, 2000 (34 minutes integration) and on January 3 and 5, 2001 (1 hour integration each). We used a  $1''$  wide slit to match the already available NIR and optical spectra and a position angle  $\text{PA}=145^\circ$ . The spectrum was acquired with an elementary integration time of 0.104 sec, while chopping

\* Based on data obtained at ESO VLT UT1 on Cerro Paranal, Chile

Send offprint requests to: L.K. Hunt

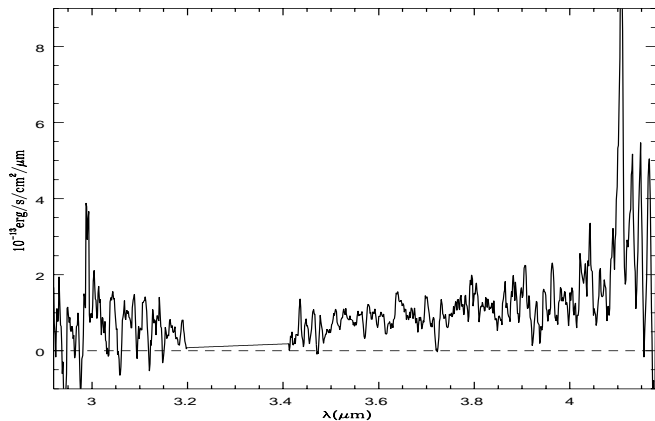


**Fig. 1.** ISAAC spectrum of SBS 0335-052. The horizontal dashed line shows the positions of zero flux, making evident the rise of the continuum toward long wavelengths. The region of poor atmospheric transmission around  $3.3\mu\text{m}$  has been removed.

with the secondary and switching (North-South) between two beams with the telescope. The telescope was dithered along the slit after each beam-switching cycle. HR 1891, a B2.5V star, was observed in the same way, in order to eliminate the telluric absorption of the atmosphere. We used the Eclipse package developed by ESO to reduce the spectra, following the standard procedures. The 2h34m combined spectrum, extracted with a  $1''$  aperture, is displayed in Fig. 1. Since the dispersion is  $14\text{\AA}/\text{pix}$ , but the slit is almost 7 pixels wide, the original spectrum has been smoothed to the effective resolution dictated by the slit. The spectrum was flux-calibrated with the photometry of our  $L'$ -band image described below.

We used the same instrument and telescope to also acquire an image in the  $L^1$  band at  $3.8\mu\text{m}$  ( $\Delta\lambda = 0.58\mu\text{m}$ ). The pixel scale was  $0.0709''/\text{pixel}$  and the total integration time 30 minutes, with an on-chip integration of 0.104 sec. Like the spectrum, the image was acquired while chopping with the secondary and nodding the telescope between the two beams. The telescope was also dithered randomly after each beam-switching cycle. We used the IRAF package for the data reduction, and relied on the telescope offsets to align the dithered images. The seeing FWHM measured from a star in the **negative** image is 6.9 pixels, or  $0.49''$ . The  $L'$  image is shown in Fig. 2.

The  $L'$ -band photometry was calibrated with the photometric standard HD 22686, obtained in the same way as the target, and assuming an  $L'$  magnitude of 7.20 (Elias et al. 1982). The growth curve of the object in the  $L'$  image is shown in the upper panel of Fig. 3; the total  $L'$  magnitude is  $14.1 \pm 0.2$ , shown as a horizontal dotted line.

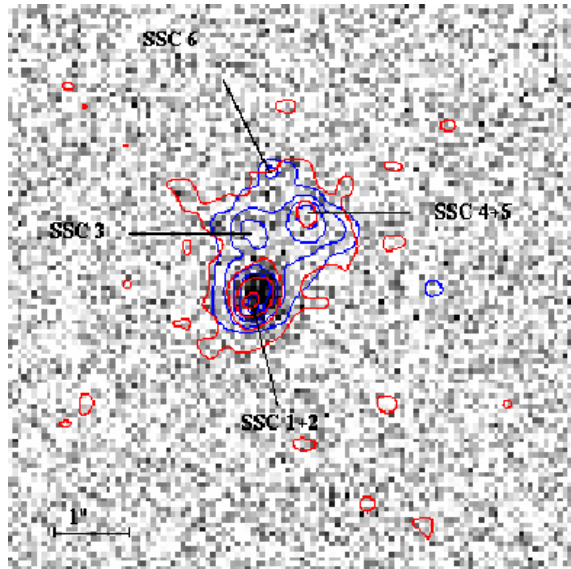


**Fig. 2.**  $L'$ -band ISAAC/VLT image with superimposed contours of the  $K_s$  image in red (VHTI), and those of the HST  $V$  image in blue (Thuan et al. 1997) (N up, E left). The SSCs denoted by Thuan et al. (1997) are also labeled.

## 2.1. Photometry and colors

SBS 0335-052 consists, as noted in the Introduction, of several SSCs superimposed on an extended blue underlying gaseous envelope. The two brightest SSC groups, SSC 1+2 and SSC 4+5 (using the notation of Thuan et al. 1997), are separated by approximately  $1.4''$ . The registration of the  $L'$  image is made difficult by the lack of field stars in the field-of-view of the direct image. Nevertheless, because of the N-S nodding direction, a relatively bright star  $\sim 26''$  E and  $52''$  S appears in the image of the negative beam. We have therefore used this star in the Digital Sky Survey (DSS) image to register the  $L'$  frame, since the star is too far away to appear in either the HST or the  $K_s$  image (VHTI). The astrometry relative to this star indicates that the  $L'$  source corresponds to the brightest SSCs, SSC 1+2, although with  $\sim 0.5\text{--}0.7''$  uncertainty because of the large pixels ( $1.7''$ ) of the DSS. Superimposed on our  $L'$  image in Fig. 2 are the contours of the HST image (blue) and the high-resolution  $K_s$  image (red).

To verify the association of the  $L'$  source with SSC 1+2, we have plotted in Fig. 3 the  $L'$  and  $K_s$  growth curves centered on SSC 1+2 and SSC 4+5, the pairs of SSCs visible in the shorter-wavelength images. Because there was no  $L'$  emission at the SSC 4+5 peak, we derived the  $L'$  photometry by fixing the position to the  $K_s$  SSC 4+5 peak. It is clear from Fig. 3 that the radial trend of the  $L'$  emission is consistent with the  $K_s$  SSC 1+2 position, since the  $L'$  emission from the SSC 4+5 is initially linear with radius, which is what is expected for no signal at the nominal center. (The SSC 4+5 curve then turns over at roughly the separation of the two SSC pairs.)

Figure 3 (lower panel) shows the  $K_s$ - $L'$  color obtained from combining our  $L'$  photometry with that from the  $K_s$

<sup>1</sup> Because of its central wavelength  $\neq 3.5\mu\text{m}$ , it is more appropriate to call this band  $L'$ , which we will do hereafter.

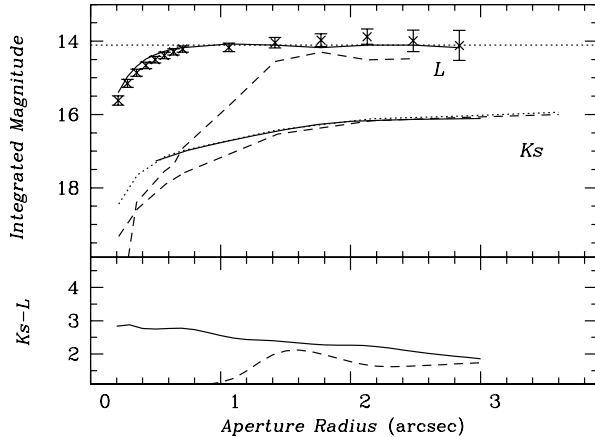


**Fig. 3.**  $L'$ -band growth curve and  $Ks-L'$  cumulative profile of SBS 0335-052. The top panel shows the data points, with respective errors, and the horizontal dotted line the total magnitude of 14.11; a solid line illustrates the growth curve for a point source on the final image. Also shown in the top panel is the  $Ks$  growth curve derived from the high-resolution  $Ks$  image in VHTI. The bottom panel shows the  $Ks-L'$  color. For all curves, the SSC 1+2 component is shown as a solid line, and SSC 4+5 as a dashed one.

image in VHTI. The  $Ks-L'$  color is extremely red, ranging from 2.8 at the center to roughly 2 for the total<sup>2</sup>. After correcting the color for our redder  $L'$  filter (see Bessell & Brett 1988), we find  $K-L$  colors of 2.1 to about 1.5 (these colors correspond to an  $L$  filter centered at  $3.5\ \mu\text{m}$ ). Such a red color is highly unusual in (non-Seyfert) extragalactic objects, and is redder than all but one of the HII galaxies studied by Glass & Moorwood (1985). Indeed, the exception, NGC 5253, has  $K-L$  colors similar to SBS 0335-052, and has been called the “youngest starburst known” by Rieke et al. (1988). Because it is also a low-metallicity dwarf galaxy, we will use NGC 5253 below as a “benchmark” for further comparisons. These colors have not been corrected for the ionized gas emission (see Section 3.2).

### 3. The dust in SBS 0335-052

The dust responsible for the  $L'$  emission appears to be *very compact*, confined to a region at most  $1.2''$  in diameter (see Fig. 3). At a distance of 54.3 Mpc (Thuan et al. 1997), this corresponds to approximately 300 pc. (This estimate is consistent with the physical extent of the ISO-emitting dust hypothesized by TSM.) The FWHM of the  $4\ \mu\text{m}$  emission is roughly equivalent to the seeing FWHM, namely  $0.5''$  or 130 pc. As seen in Fig. 3, the  $L'$  curve is very slightly more extended than a point source, but is much more compact than the  $Ks$  flux, which reaches

<sup>2</sup> Because these curves are cumulative, such a trend implies a radial blueward gradient; the  $2\ \mu\text{m}$  emission is more extended than that in  $L'$ .

its asymptotic value at a diameter of roughly 1 kpc ( $4''$ ). (SBS 0335-052 is actually more extended than this at very low  $K$  surface brightness levels, see VHTI).

#### 3.1. Extinction

Brackett  $\alpha$  in emission is clearly detected in our spectrum: we measure a flux of  $9.0 \pm 1 \cdot 10^{-15}$  erg/s/cm<sup>2</sup> in an aperture of  $1'' \times 1.5''$ . We can compare this value with the fluxes measured for  $\text{Br}\gamma$  by VHTI and  $\text{H}\beta$  by Izotov et al. (1997) in the same aperture, and use the ratio to derive the visual extinction (assuming a foreground screen). Using the intrinsic line ratios given in Osterbrock (1989) appropriate for SBS 0335-052 (Case B, 20000 K,  $400-500/\text{cm}^3$ ; Izotov et al. 1997), together with the extinction curve from Cardelli et al. (1989), we obtain from the  $\text{H}\beta/\text{Br}\alpha$  ratio  $A_V = 1.45 \pm 0.11$  mag. The  $\text{Br}\gamma/\text{Br}\alpha$  ratio gives  $A_V = 12.1 \pm 1.8$ . Izotov et al (1997) measured  $A_V = 0.55$  mag from  $\text{H}\alpha/\text{H}\beta$ , and Vanzi et al. (2000)  $A_V = 0.73$  from  $\text{H}\beta/\text{Br}\gamma$ . There is therefore a clear tendency of the extinction to increase with wavelength.

With different assumptions, recombination line ratios can be used to infer either the interstellar extinction curve, or the geometry of the obscuring dust. In the latter case, longer wavelength line ratios have the virtue of probing deeper into embedded regions, an important advantage for dusty starbursts. Following Calzetti et al. (1996), we have calculated the color excess  $E(B-V)$  derived from the hydrogen recombination lines. As before, we adopted the Cardelli et al. (1989) expression for the interstellar extinction curve, and the intrinsic line ratios from Osterbrock (1989). The color excesses are shown in Fig. 4, together with two dust models, a foreground dust screen and a homogeneously mixed slab of gas and dust. It is clear from the figure that a foreground screen model is highly inappropriate both for SBS 0335-052 ( $\times$ ) and for NGC 5253 (open circle, taken from Beck et al. 1996). It is also evident that the model of homogeneous mixed slab predicts an increase of  $A_V$  with wavelength, qualitatively similar to our observations. Nevertheless, while NGC 5253 appears to be well described by homogeneously mixed gas and dust, the low  $\text{H}\alpha/\text{H}\beta$  ratio in SBS 0335-052 together with the extremely high infrared line ratios are not well reproduced by a single value of  $\tau$  in the mixed-medium model.<sup>3</sup>

Because the extinction derived from the optical line ratios is small ( $A_V = 0.55$  mag), a more probable model consists of a nearly dustless region, responsible for virtually all of the optical emission, lying in front of a highly obscured central knot. We exclude the possibility that the interstellar extinction curve could be grossly incorrect, since we have also used the Seaton (1979) and Landini et al. (1984) curves and obtained similar results. An extinction law with a higher  $R = A_V/E(B-V)$  coupled with a mixed medium model could fit the data. Such ratios

<sup>3</sup> A clumped medium (Natta & Panagia 1984) is even worse at reproducing the observed line ratios.

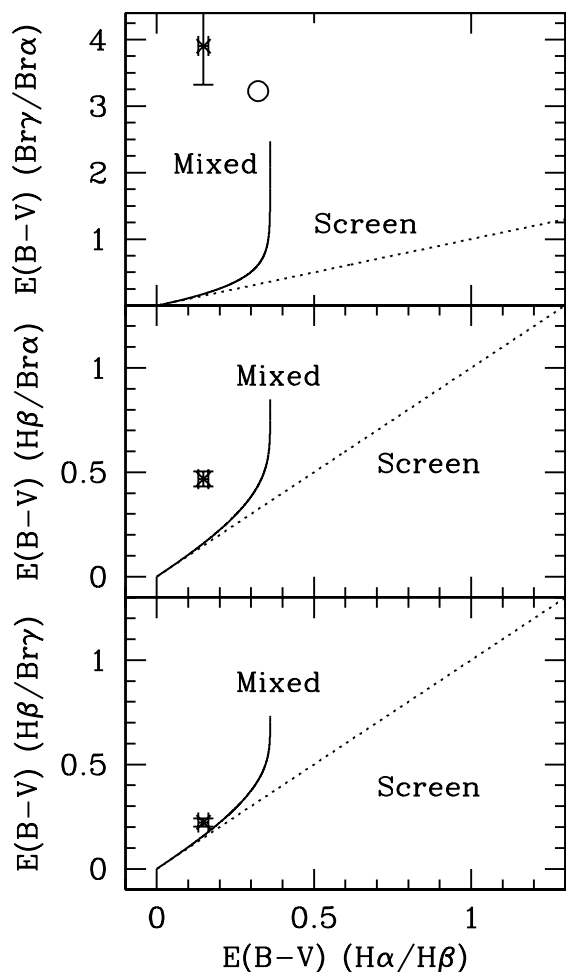


**Fig. 4.** The color excess  $E(B-V)$  derived from the hydrogen recombination line ratios; the data from SBS 0335-052 are shown as  $\times$ . Two simple models are also illustrated: the foreground screen model (labeled “Screen”) and a homogeneous mixture of gas and dust (labeled “Mixed”). The open circle shows data for NGC 5253 (Beck et al. 1996).

are typical of denser environments such as dark molecular clouds (e.g., Kim et al. 1994), but the applicability of such a law to SBS 0335-052 is not clear. Therefore, in Section 4 we will characterize the starburst in SBS 0335-052 using the simple two-component model outlined above, namely a low- $A_V$  region in front of a region highly obscured.

### 3.2. Emission

We have added new  $4\mu\text{m}$  and  $2\mu\text{m}$  points (VHTI) to the ISO spectrum of SBS 0335-052 (TSM), and fit the resulting SED. First, though, we had to estimate what fraction of the  $K$  and  $L'$  flux is due to dust. It turns out that the gas fractions determined in VHTI and below, together with reasonable estimates of stellar colors,

constrain the relative contributions of ionized gas, dust, and stars from  $1.6$  to  $4\mu\text{m}$ . The integrated  $K_s$  magnitude was used by VHTI to compare with the ISO observations obtained with a beam size larger than the galaxy; here, because of the compact  $4\mu\text{m}$  morphology, we adopt the VHTI  $K_s$  photometry for SSC 1+2 only. With the emission coefficients given in Joy & Lester (1988), and our  $\text{Br}\alpha$  observation, we find that 27% of the  $L'$  emission derives from the ionized gas continuum. Then assuming: *i*) no dust emission in  $H$  (VHTI); *ii*) stellar  $H - K \sim 0.0 - 0.2$ ; *iii*) stellar  $K - L' \sim 0.0 - 0.5$ , we derive a stellar fraction of  $\sim 37\%$  at  $2\mu\text{m}$ , compared with  $\sim 6\%$  at  $4\mu\text{m}$ <sup>4</sup>. For simplicity, we have not considered any obscuration of the stellar component. With a 50% gas fraction at  $2\mu\text{m}$  (VHTI), we therefore obtain a dust-emitting fraction of 13% at  $2\mu\text{m}$ , and 67% at  $4\mu\text{m}$ , corresponding to 0.014 mJy at  $K$  and 0.37 mJy at  $L'$ .

The combined SED from 2 to  $17\mu\text{m}$  was fit with two modified blackbodies (MBBs); the cooler one is obscured by dust in a foreground screen with an extinction curve given by Lutz (1999). As shown by TSM, this curve provides a much better fit than previous infrared extinction curves, because of its significantly higher extinction in the  $3-8\mu\text{m}$  region. The emissivity was fixed to  $\lambda^{-1.5}$  (TSM). Figure 5 shows the resulting fit; the warmer (unobscured, shown by a dashed line) MBB has a temperature of  $459 \pm 20$  K, and the cooler one (dot-dashed line)  $192 \pm 4$  K, obscured by dust with  $A_V = 16.3 \pm 0.5$  mag. These results differ slightly from VHTI, but should be more reliable because of the additional constraint of the  $4\mu\text{m}$  data point, and the use of a more refined extinction curve; also, in VHTI the emissivity was left as a free parameter, and the  $2\mu\text{m}$  flux was higher because it included emission from the whole galaxy not just SSC 1+2 (see above). In any case, the fit is very similar to that found by TSM and confirms the high extinction found by them.

Although our data suggest that the geometry is probably more a homogeneously mixed medium than a foreground screen (see Fig. 4), the comparable values of the extinction ( $A_\lambda/A_V = 0.06 - 0.08$  mag) in the MIR spectral region (Lutz 1999) make the shapes of the two fits very similar, but with  $A_V$  4 to 5 times larger in the mixed medium model. We therefore adopted the foreground screen model since it gave fits of similar, if not better, quality than the mixed medium model.

It was not possible to fit the SED with two MBBs absorbed (“extincted”) by the same amount, because the resulting fit falls off too steeply toward short wavelengths. Since the temperature and amplitude of the warm MBB are basically governed by only the 2 and  $4\mu\text{m}$  data points, an additional quantity such as extinction would not be constrained. However, the data do constrain the extinction for the warm MBB to be much smaller than that for the cool one (assuming the extinction curve is correct). Such

<sup>4</sup> The quoted values are the mean of the color range cited above.

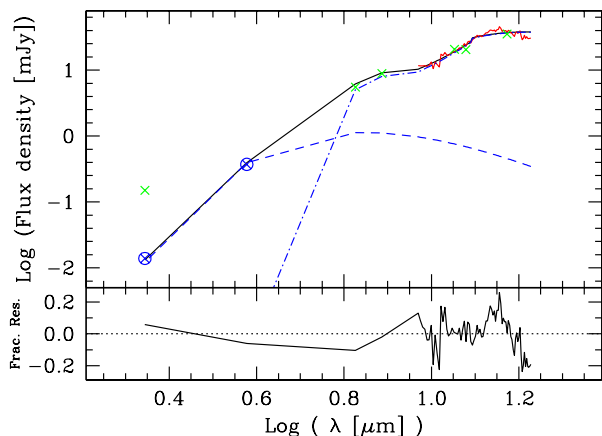


**Fig. 5.** Near- and mid-infrared SED of SBS 0335-052 with residuals from the best fit. In the upper panel, the fit is shown by a solid line, while the dashed line shows the warm modified blackbody (449 K) which is not absorbed. The dot-dashed line shows the cool modified blackbody (193 K), and affected by a foreground screen of  $A_V = 16.3$  mag. The  $2\mu\text{m}$  point lying above the fit ( $\times$ ) illustrates the  $K$  value used in VHTI, roughly 10 times higher than that adopted here. The lower panel illustrates the fractional residuals which are largest around  $12\text{--}14\mu\text{m}$ , exactly where the extinction curve is most uncertain.

a result is also consistent with the two-component model of the previous section.

### 3.3. Mass

The mid-infrared spectrum of SBS 0335-052 is unusual compared to other star-forming galaxies (e.g., Dale et al. 2001), because of its positive  $3\text{--}4\mu\text{m}$  slope, its strong continuum, and lack of spectral features (e.g., Unidentified Infrared Bands: UIBs; Polycyclic Aromatic Hydrocarbons: PAHs). Its dust properties are therefore not well described by standard dust models (Désert et al. 1990), especially regarding the very-small-grain component, and as a result we cannot plausibly estimate the mass of the *emitting* dust. Nevertheless, the extinction is likely governed by the cooler dust, and we can estimate the mass of the obscuring dust from the  $A_V$  derived from our fit of the SED.

With  $A_V = 16.3$  mag, and assuming  $N(\text{HI})/A_V \sim 2 \times 10^{21} \text{ cm}^2/\text{mag}$  and a gas-to-dust mass ratio of  $\sim 200$ , we derive a dust surface density of  $1.2 M_\odot/\text{pc}^2$ . This calculation assumes solar metallicity, but the metallicity correction factors cancel out in the end. The derived dust surface density is similar to that of the model of Draine & Lee (1984) which, with a grain opacity of  $3000 \text{ cm}^2/\text{gm}$ , is  $1.6 M_\odot/\text{pc}^2$ . If the extinction arises in a volume similar in size to the emission region (diameter  $1.2''$ ), we obtain a dust mass of  $\sim 10^5 M_\odot$ . Alternatively, we can use

the formalism of Spitzer (1978) to relate the amount of matter required to produce the observed extinction to the mean extinction curve, the density of solid material within the grain, and the grain dielectric constant (Aannestad & Purcell 1973). From the observed extinction, and assuming the grain parameters of Draine & Lee (1984), we can therefore derive the mean volume density of the dust  $\rho_d = 0.0065 M_\odot/\text{pc}^3$ , which is more than a factor of 20 higher than the Galactic value of  $0.0003 M_\odot/\text{pc}^3$ . In a spherical region of diameter  $1.2''$  as above, the dust mass becomes  $\sim 10^5 M_\odot$ , consistent with the previous estimate. These estimates are both upper limits since we have assumed a uniform distribution of the dust within the  $1.2''$  region; the actual value may be less if the dust does not extend over the entire region. These upper limits are comparable with those obtained by TSM.

## 4. Properties of the starburst

Our measurement of the  $\text{Br}\alpha$  line shows that a considerable fraction of the star formation in SBS 0335-052 is optically obscured, invisible even at  $2\mu\text{m}$ . Assuming the two-component geometry described in Section 3.1, we can adopt the (extinction corrected)  $\text{H}\beta$  flux measured by Izotov et al. (1997) to estimate the  $\text{Br}\gamma$  and  $\text{Br}\alpha$  flux originating in the same (low  $A_V$ ) region. This exercise yields values that are respectively about 50 and 25% of what is observed. That is to say, 50% of the observed  $\text{Br}\gamma$  flux and 25% of the  $\text{Br}\alpha$  comes from the (virtually) dustless foreground region which is the origin of the  $\text{H}\beta$  emission. The remaining 50% of the  $\text{Br}\gamma$  flux and 75% of  $\text{Br}\alpha$  arise in the embedded dusty star cluster; in the optical we are only observing about 1/4 of the total ionized gas emission.

The fraction of optically hidden emission can be used to estimate the extinction in the embedded cluster. We obtain  $A_V \sim 15$ , close to that inferred from the fit of the mid-infrared SED. The bright Brackett  $\alpha$  line, corrected for  $A_V \sim 15$ , indicates that the total star formation rate in the embedded cluster, instead of the optically-derived value of  $0.4 M_\odot/\text{yr}$  (Thuan et al. 1997), is more like  $\sim 1.7 M_\odot/\text{yr}$ . This last value is more than 40 times higher than that in the lowest-metallicity BCD I Zw 18 ( $0.04 M_\odot/\text{yr}$ ).

The number of massive stars in the embedded star cluster can be inferred from the the  $\text{Br}\alpha$  luminosity. With 75% of the observed  $\text{Br}\alpha$  flux coming from the obscured region, and correcting as above for  $A_V \sim 15$ ,  $L_{\text{Br}\alpha}(\text{embedded}) = 4.2 \times 10^{39} \text{ erg/s}$ . Then, using the prescription of Guseva et al. (2000), we obtain approximately  $\sim 14200$  O7 stars. There are **more than three times** as many massive stars in the embedded cluster as in the unobscured region ( $\sim 4040$ , with the observed  $L_{\text{H}\beta}$  luminosity of  $1.9 \times 10^{40} \text{ erg/s}$  in the same aperture: VHTI). The total mass of the embedded cluster can be estimated by assuming an Initial Mass Function (IMF); adopting the IMF given by Scalo (1998) gives a mass of  $1.2 \times 10^7 M_\odot$  in the embedded cluster. Alternatively, with a Salpeter IMF, and lower and upper mass cutoffs of respectively 0.8 and

$120 M_{\odot}$  (Schaerer & Vacca 1998), we obtain an embedded stellar mass of  $6.6 \times 10^6 M_{\odot}$ . The stellar density in the embedded cluster turns out to be  $\sim 85\text{--}150 M_{\odot}/\text{pc}^2$ , which is relatively low compared to the SSCs in NGC 5253 with a stellar surface density of  $\gtrsim 10^3 M_{\odot}/\text{pc}^2$  (Calzetti et al. 1997).

The massive star cluster in the obscured central knot would be expected to host a significant number of Type II supernovae (SNe). Our Br $\alpha$  measurement, together with the lowest-metallicity models of Leitherer et al. (1999), implies a SN rate of 0.004-0.006/yr, according to the stellar mass adopted (see above). We can therefore calculate the number of SNe expected to reside in the region of the SSCs, which turns out to be  $\sim 8000\text{--}12000$ , when integrated over the lifetime of the burst after the onset of SNe. If each metal-poor SN produces, on average,  $1 M_{\odot}$  of dust (Todini & Ferrara 2001), we would expect a dust mass on the order of  $10^4 M_{\odot}$ , a factor of 10 lower than the upper limit derived from the extinction. This may suggest that the dust is not spread out uniformly over the  $1.2''$  region. Also, the dust mass we infer from the extinction is highly uncertain because of the extremely low metallicity of SBS 0335-052. The physical conditions in the dense dusty medium of the embedded star cluster do not resemble those of the solar neighborhood, nor are they similar to the cold dark clouds in the Galaxy. No dust models exist for extremely low-metallicity environments; even the Magellanic Clouds modelled by Weingartner & Draine (2001) have metallicities about 4 times higher than that in SBS 0335-052. The grain properties such as the size distribution or the chemical composition may be radically different in low-metallicity environments. It is also true that even in solar-metallicity contexts the canonical models are still a subject of debate. There is evidence, for example, that a more realistic size distribution may produce the same extinction with a lower dust mass (Kim et al. 1994). Also, some fraction of grains may be “fluffy” which would also increase the extinction per unit dust mass (Krügel & Siebenmorgen 1994; Wolff et al. 1994; Mathis 1996; Snow & Witt 1996).

SBS 0335-052, while unusual for such a metal-poor object, does have peers with similar properties, although at a higher metal abundance. NGC 5253 ( $\sim 1/5 Z_{\odot}$ ) and Henize 2-10 ( $\sim 1/10 Z_{\odot}$ ) are sub-solar metallicity low-luminosity dwarf galaxies (the former a dwarf elliptical, the latter a BCD) which host powerful central starbursts with SSCs (Calzetti et al. 1997; Conti & Vacca 1994), similar to SBS 0335-052. Both galaxies show high extinction from the Brackett recombination line ratios (Beck et al. 1996, Kawara et al. 1989), but low extinction from the optical lines (see Fig. 4); they also show significant  $10 \mu\text{m}$  absorption features (Kawara et al. 1989), and host significant numbers of Wolf-Rayet stars in the central clusters (e.g., Guseva et al. 2000). Because of this and other evidence, the bursts are thought to be only a few Myr old (Beck et al. 1996; Calzetti et al. 1997; Beck et al. 1997; VHTI). In all three galaxies, the extinction is so high that optical measurements cannot be used to reliably study the

embedded star clusters; even at  $2 \mu\text{m}$  a significant fraction of the ionized gas emission is completely obscured. In the higher-metallicity objects (NGC 5253 and He 2-10), it appears that the stellar clusters are born embedded in dust and then emerge after 2–3 Myr, becoming bright in the optical and the UV (Calzetti et al. 1997). Strictly speaking, such a scenario may not be appropriate for SBS 0335-052, since, if the present burst is the first one, dust could not have predated the current episode of star formation. The quantity of dust inferred from our measurements is roughly compatible with that from primordial SN models, but the clusters themselves would have “polluted” the starburst. Either way, judging from SBS 0335-052 and its extremely low metal abundance, it is probable that much of primordial star formation could have occurred in deeply embedded dense star clusters.

## 5. Conclusions

1. We find direct evidence for a heavily absorbed central knot of star formation in SBS 0335-052. The extinction measured from the the observed Br $\gamma$ /Br $\alpha$  is  $A_V \approx 12$  mag, but line-ratio comparisons indicate that there is a virtually dust-free region along the line-of-sight to massive star clusters which are enshrouded in dust.
2. The infrared SED has been fitted with two modified blackbodies, and the inferred extinction of 16.3 mag is roughly consistent with, but slightly larger than, that obtained from Br $\gamma$ /Br $\alpha$ . The total amount of obscuring dust is estimated to be around  $10^5 M_{\odot}$ .
3. The star formation rate and number of massive stars in the embedded cluster in SBS 0335-052 are more than three times higher than inferred from optical measurements. Roughly 3/4 of the star formation in SBS 0335-052 occurs within a highly obscured embedded cluster.
4. It is likely that the SNe produced by the current burst are responsible for the dust present in SBS 0335-052, although rough estimates of their dust production are lower than the upper limits for the dust mass inferred from extinction.

*Acknowledgements.* We are especially grateful to the ESO Director General, C. Cesarsky, for the generous allocation of Director’s Discretionary Time, as well as the VLT-ISAAC staff who conducted the observations. We would like to thank Marc Sauvage who passed on the digital version of the ISO spectrum, and Dieter Lutz who gave us instantly his digital version of the Galactic extinction curve. We also acknowledge an anonymous referee for a careful reading of the manuscript and cogent comments which greatly improved the paper. TXT thanks the partial financial support of NASA-JPL Contract 961535.

## References

- Aannestad P.A., Purcell E.M. 1973, ARA&A, 309  
 Beck S.C., Turner J.L., Ho P.T.P., Lacy J.H., Kelly D.M. 1996, ApJ 457, 610  
 Beck S.C., Kelly D.M., Lacy J.H. 1997, AJ 114, 585

- Bessell M.S., Brett J.M. PASP 100, 1134
- Bohlin R.C., Savage B.D., Drake J.F. 1978, ApJ 224, 132
- Calzetti D., Kinney A.L., Storchi-Bergmann T. 1996, ApJ 458, 132
- Calzetti D., Meurer G.R., Bohlin R.C. et al. 1997, AJ 114, 1834
- Cardelli J.A., Clayton G.C., Mathis J.S. 1989, ApJ 345, 245
- Conti P.S., Vacca W.D. 1994, ApJ 423, 97
- Dale D.A., Helou G., Contursi A., Silbermann N.A., Kolhatkar S. 2001, ApJ 549, 215
- Désert F.-X., Boulanger F., Puget J.L. 1990, A&A 237, 215
- Draine B.T., Lee H.M. 1984, ApJ 285, 89
- Elias J.H., Frogel J.A., Mathews K., Neugebauer G. 1982, AJ 87, 1029
- Glass I.S., Moorwood A.F.M. 1985, MNRAS 214, 429
- Guseva N.G., Izotov Y.I., Thuan T.X. 2000, ApJ 531, 776
- Hirashita H. 1999, ApJ 522, 220
- Izotov Y. I., Lipovetsky V. A., Chaffee F. H. et al. 1997, ApJ 476, 698
- Joy M. & Lester D. F. 1988, ApJ 331, 1451
- Kim S.-H., Martin P.G., & Hendry P.D. 1994, ApJ 422, 164
- Krügel E. & Siebenmorgen R. 1994, A&A 288, 929
- Landini M., Natta A., Oliva E., Salinari P., Moorwood A.F.M. 1984, A&A 134, 284
- Leitherer C., Schaerer D., Goldader J. D., et al. 1999, ApJS 123, 3
- Lutz D. 1999, The Universe as Seen by ISO, Eds. P. Cox & M.F. Kessler, ESA-SP 427, 623
- Markarian B.E., Lipovetsky V.A., Stepanian J.A. 1983, Astrofizika 19, 29
- Mathis J.S. 1996, ApJ 472, 643
- Osterbrock D.E. 1989, *Astrophysics of Gaseous Nebulae and Active Galactic Nuclei*, University Science Books, Mill Valley
- Rieke G.H., Lebofsky M.J., Walker C.E. 1988, ApJ 325, 679
- Scalo J. 1998, ASP Conf. Series 142, 201
- Schaerer D. & Vacca W.D. 1998, ApJ 497, 618
- Seaton J.J. 1979, MNRAS 187, 73P
- Snow T.P. & Witt A. 1996, ApJ 468, 65
- Spitzer L. Jr. 1978, *Physical Processes in the Interstellar Medium*, John Wiley & Sons, Inc., New York
- Thuan T. X., Izotov Y. I., Lipovetsky V. A. 1997, ApJ 477, 661
- Thuan T. X., Sauvage M., Madden S. 1999, ApJ 516, 783 (TSM)
- Todini P., Ferrara A. 2001, MNRAS, 325, 726
- Vanzi L., Hunt L. K., Thuan T. X., Izotov Y. I. 2000, A&A 363, 493 (VHTI)
- Weingartner J.C. & Draine B.T. 2001, ApJ 548, 296
- Wolff M.J., Clayton G.C., Martin P.G., & Schulte-Ladbeck R.E. 1994, ApJ 423 412